

1 **Alternate patterns of temperature variation bring about very different disease outcomes at**
2 **different mean temperatures**

3
4 Charlotte Kunze^{1,2*}, Pepijn Luijckx^{2*#}, Andrew L. Jackson², Ian Donohue²

5
6 ¹Institute for Chemistry and Biology of the Marine Environment [ICBM], Carl-von-Ossietzky
7 University Oldenburg

8 ²Department of Zoology, School of Natural Sciences, Trinity College Dublin, Dublin, Ireland

9 *equal contribution

10 # communicating author

11

12 Keywords: Climate change, temperature variation, heatwave, host, parasite, disease, *Daphnia*,

13 *Ordospora colligata*.

14

15

16 **Abstract**

17 The dynamics of host-parasite interactions are highly temperature-dependent and may be modified by
18 increasing frequency and intensity of climate-driven heat events. Here, we show that altered patterns
19 of temperature variance lead to an almost order-of-magnitude shift in thermal performance of host and
20 pathogen life history traits over and above the effects of mean temperature and, moreover, that
21 different temperature regimes affect these traits differently. We found that diurnal fluctuations of $\pm 3^{\circ}\text{C}$
22 lowered infection rates and reduced spore burden compared to constant temperatures in our focal host
23 *Daphnia magna* exposed to the microsporidium parasite *Ordospora colligata*. In contrast, a three-day
24 heatwave ($+6^{\circ}\text{C}$) did not affect infection rates, but increased spore burden (relative to constant
25 temperatures with the same mean) at 16°C , while reducing burden at higher temperatures. We
26 conclude that changing patterns of climate variation, superimposed on shifts in mean temperatures due
27 to global warming, may have profound and unanticipated effects on disease dynamics.

28 **Introduction**

29 One of the major challenges of the 21st century is understanding how infectious diseases,
30 which have profound ecological and epidemiological impacts on human (Hotez et al., 2014),
31 agricultural (Chakraborty et al., 2011) and wildlife (Harvell et al., 2019) populations, will be affected
32 by climate change. It is now well-established that the interaction between hosts and their pathogens is
33 sensitive to temperature (Kirk et al., 2020; Rohr et al., 2013). For example, disease transmission (Ben-
34 Horin et al., 2013), host immunity (Dittmar et al., 2014; Rohr et al., 2010) and pathogen growth
35 (Gehman et al., 2018; Kirk et al., 2018) can increase with temperature, while other host-pathogen life
36 history traits such as lifespan and fecundity can decrease (Altizer et al., 2013). The interaction
37 between temperature and multiple host and pathogen life history traits highlights the inherent
38 complexity of temperature effects on infectious diseases. Indeed, each host or pathogen trait may have
39 a unique dependency on temperature and it is their combined effect (that is, R_0 , disease outbreak,
40 virulence) that is often of interest. However, while a growing body of theoretical (Kirk et al., 2020;
41 Rohr et al., 2013) and empirical (Ben-Horin et al., 2013; Dallas et al., 2016; Gehman et al., 2018; Kirk
42 et al., 2020; Zhang et al., 2019) studies have quantified the effect of rising mean temperatures on host
43 and pathogen traits (such as, for example, within-host growth (Kirk et al., 2018), pathogen
44 transmission (Kirk et al., 2019) and epidemiology (Gehman et al., 2018; Shocket et al., 2018)), the
45 influence of variable temperature regimes such as heat waves and temperature fluctuations remains
46 unresolved (Claar et al., 2020; Rohr et al., 2013).

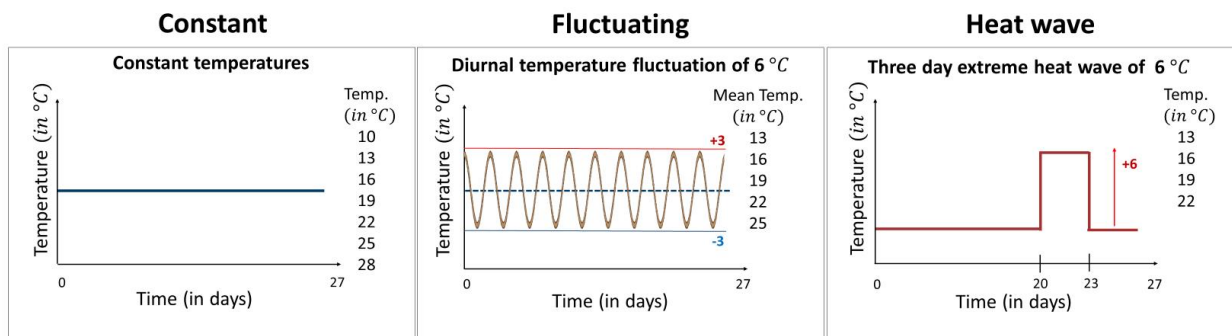
47 Climate change is predicted to increase not only mean temperatures, but also temperature
48 fluctuations and the frequency and intensity of extreme weather events (Schär et al., 2004; Vasseur et
49 al., 2014). Such changes in temperature variance have the potential to modify host-pathogen dynamics
50 (Franke et al., 2019; Rohr et al., 2013). For instance, diurnal temperature fluctuations have been
51 shown to increase malaria transmission at the lower end of the thermal range (Paaijmans et al., 2010),
52 while short-term temperature fluctuations led to reduced transmission success due to lower filtration
53 rates in a *Daphnia*-pathogen system (Dallas et al., 2016). The effect of extreme heat events on host
54 and pathogen traits is also highly variable and may depend on the magnitude, duration and intensity of
55 the applied heatwave (Landis et al., 2012; Schreven et al., 2017; Zhang et al., 2019). In a parasitoid-

56 insect interaction, a heatwave of 5 °C resulted in greater parasitoid development while a 10 °C
57 increase reduced parasitoid growth (Schreven et al., 2017). These apparent contrasting results in
58 response to variation in temperature (here used to refer both to fluctuating temperature regimes and
59 extreme heat events), imply that alternate temperature regimes or exposure to temperature shifts of
60 different magnitudes will have distinct impacts on host-pathogen interactions. Indeed, whether all
61 temperature variation acts in the same way or leads to different disease outcomes has been identified
62 as a key open question in the field (Rohr et al., 2013).

63 Here, we examine the effect of different types of temperature variation on host-pathogen
64 interactions across a broad range of mean temperatures. Specifically, we used the *Daphnia magna*—
65 *Odospora colligata* host-pathogen system to test experimentally how temperature variation alters the
66 thermal performance of both the host and the pathogen across their natural temperature range.
67 *Daphnia* are a well-established ecological model system (Miner et al., 2012) used frequently in
68 climate change studies (Dallas et al., 2016; Hector et al., 2019; Kirk et al., 2020), while *Ordospora*
69 transmission is representative of a classical environmentally-transmitted pathogen (that is, it mimics
70 diseases such as SARS-CoV-2 and *Vibrio cholerae*) and meets the assumptions of conventional
71 epidemiological models (e.g. infection following mass action (Kirk et al., 2019), continuous shedding
72 of infectious particles (Ebert, 2005) and little or no spatial structure within host populations). Our
73 microcosm experiment comprised three distinct temperature regimes: constant temperatures and two
74 variable temperature regimes with diurnal fluctuations of ± 3 °C and three-day heatwaves of six
75 degrees above ambient, all replicated over the natural temperature range of the model system (that is,
76 10-28 °C, Fig. 1). These variable temperature regimes were selected to mimic naturally-occurring
77 temperature events in habitats our study organisms encounter naturally (that is, small ponds and rock
78 pools) (Jacobs et al., 2008; Kuha et al., 2016).

79 During the experiment we measured host longevity, fecundity, infection status and the number
80 of *O. colligata* spores within the host gut (see *Methods* for details). All measurements were conducted
81 on individually-kept *Daphnia* with up to 18 replicates per measurement. To compare the three
82 different temperature regimes (that is, constant, diurnal fluctuations, heatwave; Fig. 1) we fitted a Beta
83 function (a function that can be used to capture thermal performance curves (Dowd et al., 2015)) using

84 a Bayesian framework. The advantage of using the Beta function is that each of its parameters has a
85 clear a biological meaning, where F_m is the fitness at optimal performance for the fitted host or
86 parasite trait, T_{opt} is temperature at optimal performance, and T_{min} and T_{max} are, respectively, the critical
87 minimum and maximum temperatures over which fitness of the trait becomes unviable.



88

89

90 **Fig. 1. The three temperature regimes used in the experiment.** Our experimental design comprised
91 seven constant temperature regimes with temperatures ranging from 10 °C to 28 °C, five variable
92 temperature regimes mimicking diurnal temperature fluctuations of ± 3 °C around the mean, and four
93 heatwave regimes where temperatures were identical to the equivalent constant treatment except
94 during a three-day period between days 20 and 23 when temperatures were raised by 6 °C. Constant
95 temperature regimes were replicated 12 times ($7 \times 12 = 84$ individuals), while in the variable
96 temperature regimes the number of replicates was increased to 18 as we expected increased mortality
97 in these treatments ($5 \times 18 = 90$ and $4 \times 18 = 72$, respectively for the fluctuating and heatwave
98 regime). Non-exposed controls, which received a placebo infection, were included for all treatments.
99 All animals were terminated after day 27 and fitness estimates were collected within three days.

100

101 Results

102

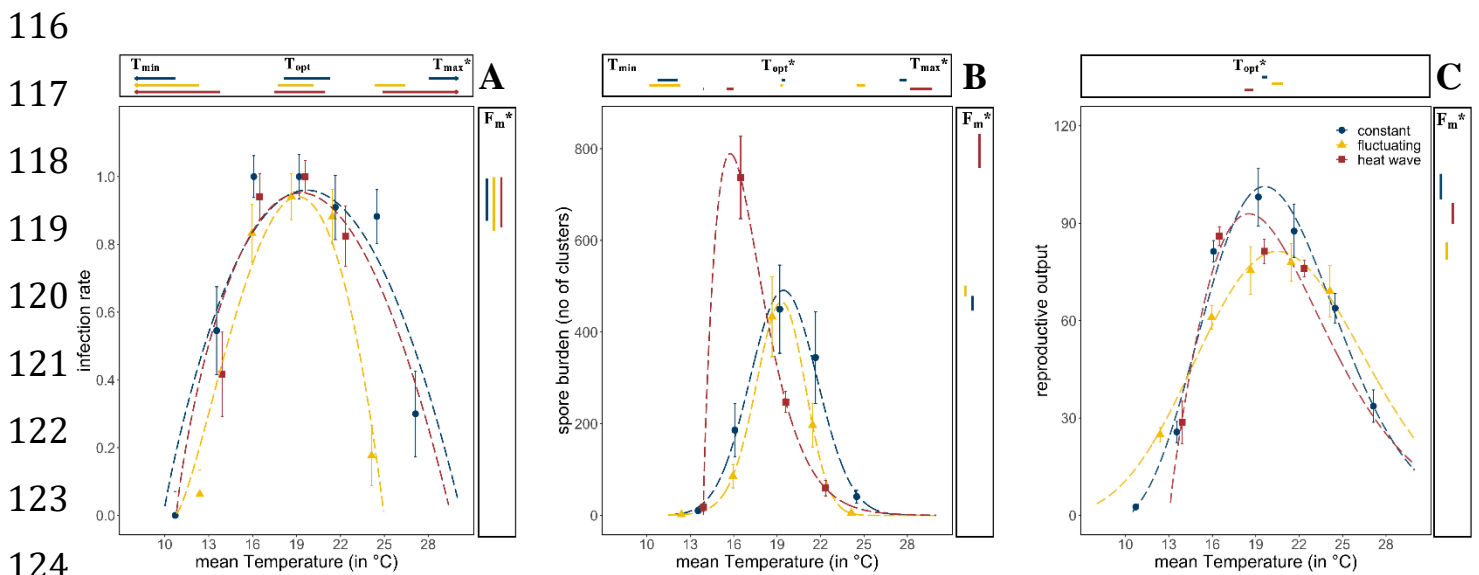
103

104

105

Diurnal temperature fluctuations narrowed the thermal performance curve for infectivity compared with constant temperatures (Fig. 2A). The maximum temperature at which spores were able to cause infections was 5 °C lower under fluctuating temperatures than under constant temperatures (Fig. 2A; $T_{max} = 25$ °C for fluctuating vs. 30 °C for constant, confidence intervals for T_{max} do not

106 overlap). The thermal performance curve for infectivity under the heatwave, where temperatures were
 107 raised by 6 °C for three days and then returned to constant temperature (Fig. 1), was almost identical
 108 to that under constant temperature (all confidence intervals overlap, Fig 2A & Table S2). However,
 109 unlike the constant temperature regime, the heatwave did not differ from the fluctuating regime, as
 110 estimates for the maximum temperature had broad confidence intervals, likely caused by the lack of
 111 data at the higher temperatures. Remaining parameter estimates of the Beta Equation were similar for
 112 the three temperature regimes, with the highest rate of infection at 19 °C, a maximum infection rate of
 113 ~95% infection and no infections under 10 °C (Fig. 2A & Table S2; confidence intervals overlap for
 114 T_{opt} , F_m and T_{min}). Thus, while diurnal fluctuations led to less infection at higher temperatures, a
 115 heatwave did not alter infection rates.



125 **Fig. 2. Thermal performance curves of host and parasite life history traits across our three**
 126 **temperature regimes.** (a) Infection rates of *Ordospora* in its *Daphnia* host. (b) Mean number of spore
 127 clusters in infected *Daphnia* at the end of the experiment. (c) Reproductive output of the host when
 128 exposed to *Ordospora* (for a comparison of unexposed and exposed individuals see Fig. 3). For all
 129 panels the constant temperature regime is in blue, the diurnally fluctuating regime in yellow and the
 130 heatwave in red. Points present the observed mean values for the measured traits and dashed lines
 131 provide the fit for the Beta Equation. 95% confidence intervals of minimum, optimal and maximum
 132 temperature estimates (respectively, $T_{min}/T_{opt}/T_{max}$) are shown above the x-axis. The estimate for the
 133 optimal value of the life history trait (F_m) and its 95% confidence interval is displayed to the right of

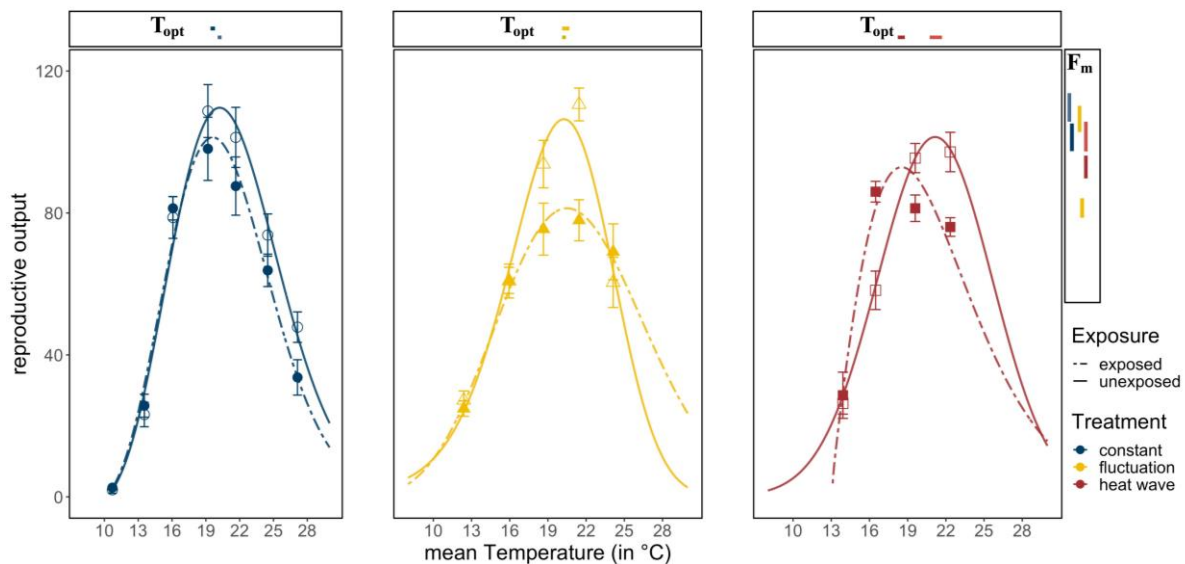
134 *each panel. Significant differences (non-overlapping 95% confidence intervals) in parameter*
135 *estimates are highlighted with an asterisk. Error bars on data points indicate standard error. Beta*
136 *Equation parameter estimates displayed in this figure can be found in tables S2-S4.*

137

138 Spore burden of the two variable temperature regimes deviated from both the constant
139 temperature regime and from each other (Fig. 2B). Consistent with infection rates, daily temperature
140 fluctuation led to a lower maximum temperature (by ~ 3 °C) for parasite growth within the host,
141 resulting in a narrowed thermal performance curve for burden compared with the other temperature
142 regimes (Fig 2B & Table S3, non-overlapping confidence intervals for T_{\max}). This is supported further
143 by the consistently lower spore burden for the fluctuating regime when compared with the constant
144 temperature regime except near the optimum temperature of 19 °C, where spore burdens of both
145 temperature regimes were similar (confidence intervals for T_{opt} and F_m overlap). While infection rates
146 and burden showed a similar thermal performance for diurnal fluctuations (both narrowing), the
147 response to the heatwave differed between infection and burden (Fig. 2). Compared to the constant
148 temperature regime spore burden in the heatwave showed a shift in the optimum temperature (from
149 19.4°C to 15.7°C), and an increase in the number of spore clusters (Fig. 2B, confidence intervals for
150 T_{opt} , and F_m do not overlap). However, while spore burden was different at ~ 16 °C, at ~ 19 °C spore
151 burden was nearly identical for all three temperature regimes. Moreover, due to the opposite effects at
152 16 °C for both variable temperature regimes (that is, a narrowing of performance under fluctuating
153 temperatures, exacerbation under heatwave) spore burden at this temperature differed by almost an
154 order of magnitude (that is, 86 vs. 737 spore clusters).

155 Host fitness was generally reduced when exposed to *Ordospora* spores or when experiencing variable
156 temperature regimes. *Daphnia* exposed to the parasite had lower reproductive success near the
157 optimum temperature (~ 20 °C) compared to unexposed controls (non-overlapping confidence intervals
158 for F_m) and lost between 8% (constant) and 24% (diurnal fluctuation) of reproductive output (Fig. 3).
159 Comparing host performance among the different temperature regimes shows that exposed animals in
160 variable temperatures had lower reproductive success (Fig. 2C & Table S4, non-overlapping 95%
161 intervals for F_m), with a small shift (1.1 °C) in their thermal optimum under the heatwave regime (Fig.

162 2C, non-overlapping 95% intervals for T_{opt}). Unexposed animals also had lower fitness when
 163 experiencing the heatwave (Fig. 3, non-overlapping 95% intervals for F_m) and, while the reproduction
 164 at the optimal temperature of the unexposed animals experiencing diurnal fluctuations was lower,
 165 confidence intervals overlapped with the constant temperature regime (Fig 3). The host response to the
 166 variable temperature regimes differed from that of the pathogen (compare thermal performance curves
 167 for the heatwave and diurnal fluctuating regimes between figures 2A, B & C). While host performance
 168 was reduced (lower F_m) under both variable temperature regimes, parasite traits showed either a
 169 narrowing of the performance curve (for diurnal fluctuations) or no effect and greatly increased
 170 performance (for infection and burden under the heatwave).
 171



172
 173 **Fig. 3. Reproductive success in exposed and unexposed *Daphnia*.** Exposed *Daphnia* (dotted lines)
 174 produce less offspring than unexposed individuals (solid lines). Lines are the fitted Beta Functions for
 175 the different temperature regimes (constant temperature regime in blue, the diurnally fluctuating
 176 regime in yellow and the heatwave in red). 95% confidence intervals of reproductive output (F_m) are
 177 shown to the right, and the temperature where it is at its optimum (T_{opt}), are shown above the x-axis.
 178 Significant differences in parameter estimates of the Beta Function are highlighted with an asterisk.
 179 Estimates for minimum and maximum temperatures are not displayed as we used restrictive priors.
 180 Error bars on data points indicate standard error. Beta Equation parameter estimates displayed in
 181 this figure can be found in table S4.

182
183 **Discussion**

184 We show that not only does temperature variation alter the thermal performance of host and
185 pathogen life history traits in a unique way, driving a shift in performance up to order-of-magnitude
186 over and above the effect of mean temperature, but that the type of variation and the mean temperature
187 at which it occurs are also critical. Indeed, each of the life history traits we measured was affected
188 differently by thermal variation. While variable temperature regimes affected host and pathogen
189 performance, the direction and strength of this depended both on the type of variation and the mean
190 temperature to which it was applied. With global warming altering the mean and variance of
191 temperature around the world, how this affects diseases and their dynamics is a critical outstanding
192 question (Claar et al., 2020; Rohr et al., 2013). Our results demonstrate that the combined effect of
193 changing temperature mean and variance can be highly complex, and may alter the vulnerability of
194 host populations (Harvell et al., 2019), affect the evolution of host and parasites (Buckley et al., 2016)
195 and, therefore, impede our ability to accurately predict future disease outbreaks.

196 Infection rates were reduced at higher temperatures when animals experienced diurnal
197 fluctuations but not after experiencing a heatwave. In *Daphnia*, filtration rates determine the contact
198 rate between host and pathogen, and a reduction in filtration can thus lead to reduced levels of
199 infection (Hall et al., 2010). As filtration rates of *Daphnia magna* decline at higher temperatures (Kirk
200 et al., 2019), average infection rates under diurnal temperature fluctuations would thus be expected to
201 be lower due to the non-linear nature of the thermal performance curve (that is, Jensen's inequality
202 (Dowd et al., 2015)). In addition, infection probability in our study system decreases sharply when
203 temperatures surpass 22 °C (Kirk et al., 2019), reducing infection rates under fluctuating temperatures
204 that exceed this temperature (again, due to Jensen's inequality). In systems where immune function
205 depends on temperature (e.g. insects, mosquitos and ectotherms in general (Paaijmans et al., 2013),
206 heatwaves may interact with the immune system in complex ways (Murdock et al., 2012), particularly
207 when the heatwave occurs early in the infection process. However, given that our heatwave occurred
208 twenty days post-infection and that *Daphnia* are not known to recover from infection (Ebert, 2005),
209 the effect of the heatwave on established infections may have been limited. Absence of an effect of a
210 heatwave on infection rates has also been found for a pipefish-trematode host-parasite system (Landis

211 et al., 2012). However, though the heatwave did not affect infection rates in our experiment, it did
212 affect parasite burden.

213 Our results show that different types of temperature variation can alter parasite burden and
214 thus affect pathogen growth within the host. While diurnal temperature fluctuations and heatwaves
215 brought about an almost order of magnitude difference in spore burden at a mean temperature of 16
216 °C, no differences were observed at ~19 °C. Generally, similar to infection rates, the thermal
217 performance curve for spore burden narrowed under fluctuating temperatures, as predicted by
218 averaging over the non-linear thermal performance curve (Denny, 2017; Dowd et al., 2015). The
219 impact of diurnal temperature fluctuations on parasite fitness has been studied previously, with
220 multiple studies suggesting a shift in the thermal performance of parasite fitness under fluctuating
221 temperatures (Dallas et al., 2016; Duncan et al., 2011; S. E. Greenspan et al., 2017; Paaijmans et al.,
222 2010). Indeed, our findings that *Ordospora* has a narrower thermal performance for spore burden and
223 infectivity under fluctuating temperatures adds to a growing body of evidence (Dallas et al., 2016; S.
224 E. Greenspan et al., 2017; Hector et al., 2019; Roth et al., 2010) suggesting that estimates and
225 predictions that ignore temperature variation may over- or underestimate disease burden and
226 prevalence (Sasha E. Greenspan et al., 2017; Raffel et al., 2013; Rohr et al., 2013). Moreover, with
227 almost an order-of-magnitude difference between both our two variable temperature regimes at some
228 — though not all — temperatures, our results highlight that both the context and type of temperature
229 variance needs to be considered when trying to understand how pathogen performance may be
230 affected by climate change.

231 Spore burden increased following heatwaves, but the effect depended on the mean
232 temperature to which the heatwave was applied. Indeed, the heatwave had either higher, similar or
233 lower spore burden compared to the equivalent constant temperature regime. It was shown recently in
234 a fish-tapeworm host-parasite system that parasite growth, egg production and the number of first-
235 stage larvae increased after a one-week exposure to higher temperatures (increase up to 7.5 °C)
236 (Franke et al., 2019). Our findings corroborate that heatwaves associated with climate change may,
237 under some conditions, increase disease burden. Indeed, we found a considerable increase in spore
238 burden and a shift in the optimum temperature following a three-day increase in temperature of 6 °C at

239 16 °C. Although some studies have reported increased disease susceptibility following heatwaves
240 (Dittmar et al., 2014; Roth et al., 2010), others found no effect on immune function (Stahlschmidt et
241 al., 2017) or reduced disease performance after exposure to high temperatures (Fayer et al., 1998). Our
242 results may explain these conflicting findings — we found that the effects of a heatwave on spore
243 burden are contingent on the mean temperature to which the heatwave is applied. That is, our results
244 show that the heatwave has either lower or higher burden than equivalent constant temperatures. This
245 context-dependency of heatwaves is supported further by studies in both plant-endoparasite (Schreven
246 et al., 2017) and herbivore-parasitoid (Zhang et al., 2019) systems, which showed that the effect of a
247 heatwave on parasite traits depended on the amplitude of the extreme event. As highlighted by a recent
248 review (Claar et al., 2020), effects of warming events on disease traits remain difficult to generalise,
249 and more studies and insight into underlying principles and mechanisms is needed to forecast the
250 effect of extreme heat events on disease dynamics. Indeed, while it is clear from our experiment that a
251 short, three-day increase in temperature can drastically alter the thermal performance curve for
252 parasite burden, the exact mechanism(s) underlying this change remains unidentified.

253 Differences in acclimatisation speeds between hosts and pathogens may explain the observed
254 increase in burden of *Ordospora* at 16 °C following a heatwave. According to the temperature
255 variability hypothesis (Raffel et al., 2013; Rohr et al., 2013), parasites, which have faster metabolic
256 rates due to their smaller size, should acclimatise more rapidly to changing temperatures than their
257 larger hosts. In unpredictable variable environments, such as our heatwave regime, parasites thus
258 should have an advantage over their hosts. Moreover, host resistance may also decrease as a result of a
259 trade-off between the energy demand for acclimatisation and immunity (Nelson et al., 1996). That
260 varying temperature can lead to higher infection prevalence has been established in Cuban tree frogs,
261 red-spotted newts and abalone (Ben-Horin et al., 2013; Raffel et al., 2013). While this hypothesis may
262 explain our observation of high burden for the heatwave near 16 °C, it does not, however, explain why
263 the response depends on the mean (that is, lower performance at higher temperatures). Though
264 *Ordospora* should have an overall advantage under the temperature variability hypothesis, the realised
265 advantage may be smaller as its thermal range is more restricted than its host (Kirk et al., 2018). The
266 heatwave may thus cause proportionally more stress in the parasite than the host at high temperatures,

267 consistent with the thermal stress hypothesis, which suggests that a shift in temperature may reduce
268 performance of either host or parasite (Paull et al., 2015). Indeed, that thermal stress can affect host
269 and pathogen performance has been well supported (Gehman et al., 2018; Kirk et al., 2019; Schreven
270 et al., 2017; Zhang et al., 2019). Alternatively, the observed increase in parasite burden due to
271 heatwaves may be system-specific and not explained by differences in acclimatisation speed.
272 Estimates show that growth rates of *Ordospora* increase by a factor of five between 20 °C and 24 °C
273 before declining again (Kirk et al., 2018). While the optimal performance of *Ordospora* occurs around
274 19 °C, due to the balance of thermal performance curves of other host and pathogen traits (e.g.
275 mortality, infectivity, etc), a temporary increase to 22 °C, as occurred under our heatwave at 16 °C,
276 may thus have exacerbated pathogen growth, particularly if different traits react differently to a
277 temperature disturbance, which may have disrupted the balance between host and parasite.

278 Changes in host fecundity in response to temperature variation differed to the response of both
279 parasite traits (that is, infectivity and spore burden) we measured. While infectivity and burden had
280 either a narrower thermal performance curve or showed a heightened and shifted peak, temperature
281 variation lowered reproductive output of the host near the thermal optimum. A reduction in
282 reproductive output of the host under variable temperatures is consistent with previous work both on
283 *Daphnia* (Schwartz et al., 2016) and in other systems (Craig et al., 1983; Uvarov et al., 2011).
284 Similarly, a reduction in host fecundity due to parasitism is well established (Ebert, 2005). Infection
285 may also reduce the thermal tolerance of the host (Hector et al., 2019), which would explain the small
286 shift of the thermal optimum for host reproduction under the heatwave regime. While host responses
287 are thus consistent with expectations, the distinct responses to the different temperature regimes of the
288 different life history traits we measured (that is, host fecundity, parasite infectivity and parasite
289 burden) highlight that the effects of temperature variation on host-pathogen systems are complex.
290 When trying to model disease dynamics and outbreaks, we often include a multitude of host and
291 pathogen traits, each with their own thermal dependencies. Recent studies have made advances in
292 predicting disease growth and spread under rising mean temperatures, integrating approaches and
293 identifying mechanisms that can capture and predict the thermal performance of host and pathogen
294 traits within epidemiological models (e.g., metabolic theory) (Kirk et al., 2020). It remains to be seen,

295 however, whether such modelling frameworks can be extended to incorporate temperature variation,
296 especially considering the distinct responses for the life history traits we measured to each of our
297 variable temperature regimes.

298 Our study shows that temperature variation alters the outcome of host-pathogen interactions in
299 complex ways. Not only does temperature variation affect different host and pathogen life history
300 traits in a distinct way, but the type of variation and the mean temperature to which it is applied also
301 matters, with up to an order of magnitude change between diurnal fluctuations in temperature and
302 extreme heat events. With global warming altering both the mean and variance of temperature around
303 the world, we can thus expect to see unanticipated changes in disease dynamics of host-pathogen
304 systems. Indeed, extreme temperature events like *El Niño* have been linked to disease-driven collapses
305 of keystone predators (Harvell et al., 2019), increases in diseases such as dengue and cholera
306 (Anyamba et al., 2019), and shifts in the geographic distribution of pathogens (Claar et al., 2020).
307 While temperature variation can thus affect disease dynamics in human, wildlife and livestock
308 populations — with potentially devastating economic and health consequences (Altizer et al., 2013) —
309 the complexity of the effects of temperature and its variation currently limits our ability to move
310 beyond system-specific predictions, in particular for extreme temperature events (Claar et al., 2020).
311 We conclude that improving our mechanistic understanding of the role of temperature variation on
312 disease dynamics, and exploring the generality of its effects and how it affects thermal performance
313 curves of both hosts and parasites (Claar et al., 2020), are critical to predicting disease dynamics in a
314 warming world.

315

316 **Materials and Methods**

317 *Study system*

318 The crustacean *Daphnia magna* plays a key role in ecosystem functioning. *Daphnia* are filter
319 feeders that consume planktonic algae and other microorganisms, thus promoting water transparency
320 and helping to prevent algal blooms (Miner et al., 2012). They are a key food source for planktivorous
321 fish and thus constitute a major part in the food web (Ebert, 2005) and play a key role in nutrient
322 cycling (Elser et al., 2000). Over its entire range, *Daphnia* is affected by a broad variety of pathogens.

323 Here, we use *Odospora colligata*, a widely distributed microsporidium parasite that is only known to
324 infect *Daphnia magna*. This gut parasite has been recently used as a model to understand how changes
325 in mean temperatures under global warming may affect host-parasite systems (Kirk et al., 2020).
326 However, effects of temperature variance remain unstudied. *Daphnia* become infected when they
327 accidentally ingest water borne spores of *Odospora* while filter feeding. After successful establishment,
328 spores divide intracellularly in the gut epithelium of *D. magna* (Larsson et al., 1997) until they form a
329 cluster of 32 to 64 spores. Spores are then released either to the environment or go on to infecting
330 neighbouring cells after *O. colligata* lyses the cell.

331 332 *Experimental set-up*

333 In the laboratory, we established water baths with temperatures ranging from 10 – 28 °C. Each
334 bath was regulated with a temperature controller (Inkbird ITC-308) that interfaced with cooling
335 (Hailea HC300A) and heating (EHEIM JÄGER 300W) units. Pumps (Micro-Jet Oxy) were used to
336 create constant flow, which ensured equal temperature distribution within the water baths. Each bath
337 held up to 99 microcosms and was kept under natural lighting conditions (16:8 light:dark).
338 Temperature and light intensity were recorded using HOBO loggers which were housed in the spare
339 microcosms. Each microcosm was filled with up to 80 ml of Artificial *Daphnia* Medium (ADaM,
340 modified to use only 5% of the recommended seleniumdioxide concentration (Klüttgen et al., 1994)).

341 To test for the effect of changing both mean temperature and patterns of temperature variation
342 in our host-parasite system, we created three different temperature regimes: one constant and two
343 variable temperature regimes, the latter comprising diurnal temperature fluctuations and a heatwave
344 (Fig. 1). In the constant temperature regime, individual *Daphnia* were kept at one of seven
345 temperatures for the whole experimental period (that is, 10, 13, 16, 19, 22, 25 and 28 °C). The diurnal
346 fluctuation regime comprised five temperature levels, which experienced the same mean temperature
347 as the constant regimes but with a fluctuation of ± 3 °C every 12 hours (that is, 10 – 16 °C, 13 – 19 °C,
348 16 – 22 °C, 19 – 25 °C, 22 – 28 °C), mimicking diurnal fluctuations in small rock pools (Jacobs et al.,
349 2008). The heatwave was performed at four different temperature levels (13, 16, 19, 22 °C), with
350 conditions identical to the constant regime except for an increase of 6°C for 72 hours, 20 days after
351 animals were exposed to the parasite, mimicking a short heatwave (Kuha et al., 2016). We chose these

352 temperature levels because of their relevance for our host and pathogen system, as no infection occurs
353 below 12 °C and hosts have high mortality above 30 °C (Kirk et al., 2018, 2019). Animals were kept
354 individually in microcosms, organised into trays and repositioned daily to avoid positioning effects. In
355 each temperature regime half of the microcosms were exposed to the parasite while the other half
356 served as controls. For each of the constant temperature levels, we used 12 replicates for both exposed
357 and control animals. However, as we expected increased mortality in the variable temperature regimes
358 (Régnière et al., 2012), we increased the number of replicates of these regimes to 18. We based this
359 number of replicates on experience with previous temperature experiments with the *Daphnia*-
360 *Ordospora* system (Kirk et al., 2019).

361 The *Daphnia* genotype (clone FI-OER-3-3) we used was previously isolated from a rock pool
362 at Tvärminne archipelago, Finland and propagated clonally in the laboratory. To generate sufficient
363 animals for the experiment, we grew *Daphnia* asexually under standardized conditions for three
364 weeks. Animals were raised in small populations (twenty 400 ml microcosms, 12 animals per
365 microcosm) under continuous light at 20 °C. The medium (ADaM) was replaced at least twice a week
366 and *Daphnia* were fed *ad libitum* with *Scenedesmus* algae (*Scenedesmus* sp.), which was grown in
367 batch cultures at 20 °C in WC Medium (Kilham *et al.*, 1998) under nutrient- and light-saturated
368 conditions. The experiment was initiated by collecting a cohort of female juveniles (~600 females up
369 to 72 hours old) from the small population microcosms. Individual juveniles were then randomly
370 transferred into 100 ml glass microcosms filled with 40 ml ADaM. These glass microcosms were
371 placed into their assigned water baths and, after an acclimation period of 24 hours, the animals were
372 exposed to the parasite by adding 1 ml medium containing ~10000 spores of *O. colligata*. This spore
373 solution was prepared by crushing 3560 infected *D. magna* individuals with known average burden
374 (determined by using phase contrast microscopy on a sub-sample), using mortar and pestle and
375 diluting down the resulting spore slurry. The unexposed controls received a placebo exposure
376 consisting of crushed uninfected animals diluted in medium. Animals were exposed either to the
377 parasite or placebo for six days and were transferred subsequently to clean microcosms with fresh
378 medium (80 ml of ADaM) twice a week until the end of the experiment. Animals were fed four times
379 a week with increasing amount of algae to accommodate the increased food demand of the growing

380 animals (from 4 million algae ml⁻¹ at the start of the experiment to 10 million algae ml⁻¹ by day ten
381 which was maintained until the end of the experiment). Between transfers, evaporation of the medium
382 was offset by refilling microcosms daily with 50-50 ADaM-distilled water.

383
384 *Measurements of host and parasite life history traits*

385 To obtain fitness estimates for the host, we counted the offspring produced and checked
386 mortality of all animals daily. Infection status and spore burden (that is, the number of spores inside
387 the host) were assessed upon death by dissecting individuals and counting the number of spore clusters
388 (each cluster holds up to 64 parasite spores) in the gut with phase contrast microscopy (400x
389 magnification). Any animals that remained alive until the end of the experiment (day 27) were
390 terminated within three days, dissected and their infection status and burden were determined without
391 the observer being aware of the identity of the sample. Because infections cannot be diagnosed
392 accurately in early infection stages, animals that died before day 11 were not considered in analyses.
393 Any male *Daphnia* that were misidentified as female at the start of the experiment were also excluded.
394 In addition, to prevent potentially confounding effects of animals that died early (where the parasite
395 had less time to grow) as having lower spore burden, we included only animals from the last day of
396 the experiment in the analysis for spore burden. Note that, to facilitate good estimates for spore
397 burden, we terminated most hosts before natural death occurred, which limits our ability to assess the
398 effects of virulence (host mortality, reduced fecundity).

399 *Data analysis*

400 Analyses were performed using R version 3.6.1 (R Core Team, 2018) interfacing with JAGS
401 (Lunn et al., 2009; Plummer et al., 2006), and used datafiles and code are available at
402 <https://github.com/charlyknz/HostParasite.git>. A Beta Function was fitted to each of our different
403 fitness estimates (that is, host fecundity, parasite infectivity and burden) for each of the three
404 temperature regimes, as:

$$f = F_m \left(\frac{T_{max} - T}{T_{max} - T_{opt}} \right) \left(\frac{T - T_{min}}{T_{opt} - T_{min}} \right)^{\left(\frac{T_{opt} - T_{min}}{T_{max} - T_{opt}} \right)}$$

405 where f is fitness at temperature T , F_m is estimated fitness at optimal performance for the fitted host or
406 parasite trait, T_{opt} is temperature at optimal performance, and T_{min} and T_{max} are, respectively, the critical
407 minimum and maximum temperatures over which fitness of the trait becomes unviable. This non-
408 linear function has been shown to capture thermal performance accurately (Niehaus et al., 2012) and
409 has the advantage that all four parameters in the equation have clear biological meaning.

410 To determine the effect of both mean and variation in temperature on host and pathogen traits,
411 we used a Poisson distribution for reproductive output (number of offspring per individual) and spore
412 burden (number of spore clusters produced by the parasite). For pathogen infectivity we used a
413 binomial distribution. Models were fitted using the MCMC fitting algorithm called from R. All
414 models were fitted in a Bayesian framework with JAGS (Lunn et al., 2009; Plummer et al., 2006),
415 while allowing for separate parameter values for each of the different temperature regimes. Priors for
416 temperature effects were specified in order to satisfy the necessary condition $T_{min} \leq T_{opt} \leq T_{max}$ and
417 informed by previous work (See Table S1 for the priors) (Kirk et al., 2018, 2019, 2020). The posterior
418 distribution of all parameters was estimated using 3 chains, 10000 posterior draws which were then
419 thinned by five to yield 6000 samples ($3 \times 10000 / 5$). Model convergence was checked using the
420 Gelman-Rubin diagnostic.

421

422

423 **Acknowledgements**

424 We thank Dieter Ebert and Jürgen Hottinger for provision of the biological materials, Alison Boyce
425 for technical assistance in creating the water baths and Maren Striebel for helpful comments on the
426 manuscript. ALJ was funded by an Irish Research Council grant IRCLA/2017/186. PL was funded by
427 a Science Foundation Ireland Frontiers for the Future grant 19/FFP/6839. The authors have no
428 conflicts of interest to declare.

429

430 **Author contributions**

- 431 CK, PL and ID designed the experiment. CK and PL conducted the experiment with assistance of ID.
- 432 ALJ, CK and PL conducted the analyses. CK and PL wrote the first draft of the manuscript and all
- 433 authors contributed to revisions.

- 434 Altizer, S., Ostfeld, R. S., Johnson, P. T. J., Kutz, S., & Harvell, C. D. (2013). Climate change and
435 infectious diseases: From evidence to a predictive framework. *Science*, *341*(6145), 514–519. doi:
436 10.1126/science.1239401
- 437 Anyamba, A., Chretien, J. P., Britch, S. C., Soebiyanto, R. P., Small, J. L., Jepsen, R., Forshey, B. M.,
438 Sanchez, J. L., Smith, R. D., Harris, R., Tucker, C. J., Karesh, W. B., & Linthicum, K. J. (2019).
439 Global disease outbreaks associated with the 2015–2016 El Niño event. *Scientific Reports*, *9*(1),
440 1–14. doi: 10.1038/s41598-018-38034-z
- 441 Ben-Horin, T., Lafferty, K., & Lenihan, H. S. (2013). Variable intertidal temperature explains why
442 disease endangers black abalone. *Ecology*, *94*(1), 161–168. doi: 10.2307/23435678
- 443 Buckley, L. B., & Huey, R. B. (2016). How extreme temperatures impact organisms and the evolution
444 of their thermal tolerance. *Integrative and Comparative Biology*, *56*(1), 98–109. doi:
445 10.1093/icb/icw004
- 446 Chakraborty, S., & Newton, A. C. (2011). Climate change, plant diseases and food security: an
447 overview. *Plant Pathology*, *60*(1), 2–14. doi: 10.1111/j.1365-3059.2010.02411.x
- 448 Claar, D. C., & Wood, C. L. (2020). Pulse heat stress and parasitism in a warming world. *Trends in*
449 *Ecology and Evolution*, *35*(8), 704–715. doi: 10.1016/j.tree.2020.04.002
- 450 Craig, J. F., & Kipling, C. (1983). Reproduction effort versus the environment; case histories of
451 Windermere perch, *Perca fluviatilis* L., and pike, *Esox lucius* L. *Journal of Fish Biology*, *22*(6),
452 713–727. doi: 10.1111/j.1095-8649.1983.tb04231.x
- 453 Dallas, T., & Drake, J. M. (2016). Fluctuating temperatures alter environmental pathogen transmission
454 in a *Daphnia*–pathogen system. *Ecology and Evolution*, *6*(21), 7931–7938. doi:
455 10.1002/ece3.2539
- 456 Denny, M. (2017). The fallacy of the average: On the ubiquity, utility and continuing novelty of
457 Jensen’s inequality. *Journal of Experimental Biology*, *220*(2), 139–146. doi: 10.1242/jeb.140368
- 458 Dittmar, J., Janssen, H., Kuske, A., Kurtz, J., & Scharsack, J. P. (2014). Heat and immunity: An
459 experimental heat wave alters immune functions in three-spined sticklebacks (*Gasterosteus*
460 *aculeatus*). *Journal of Animal Ecology*, *83*(4), 744–757. doi: 10.1111/1365-2656.12175
- 461 Dowd, W. W., King, F. A., & Denny, M. W. (2015). Thermal variation, thermal extremes and the

- 462 physiological performance of individuals. *Journal of Experimental Biology*, 218(12), 1956–
463 1967. doi: 10.1242/jeb.114926
- 464 Duncan, A. B., Fellous, S., & Kaltz, O. (2011). Temporal variation in temperature determines disease
465 spread and maintenance in paramecium microcosm populations. *Proceedings of the Royal
466 Society B: Biological Sciences*, 278(1723), 3412–3420. doi: 10.1098/rspb.2011.0287
- 467 Ebert, D. (2005). *Ecology; epidemiology; and evolution of parasitism in Daphnia [Internet]*. Bethesda
468 (MD): National Library of Medicine (US); National Center for Biotechnology Information.
- 469 Elser, J. J., Fagan, W. F., Denno, R. F., Dobberfuhl, D. R., Folarin, A., Huberty, A., Interlandi, S.,
470 Kilham, S. S., McCauley, E., Schulz, K. L., Siemann, E. H., & Sterner, R. W. (2000). Nutritional
471 constraints in terrestrial and freshwater food webs. *Nature*, 408(6812), 578–580. doi:
472 10.1038/35046058
- 473 Fayer, R. ., Trout, J. . M. ., & Jenkins, M. C. (1998). Infectivity of microsporidia spores stored in
474 water at environmental temperatures. *J. Parasitol.*, 84(6), 1165–1169.
- 475 Franke, F., Raifarh, N., Kurtz, J., & Scharsack, J. P. (2019). Consequences of divergent temperature
476 optima in a host–parasite system. *Oikos*, 128(6), 869–880. doi: 10.1111/oik.05864
- 477 Gehman, A. L. M., Hall, R. J., & Byers, J. E. (2018). Host and parasite thermal ecology jointly
478 determine the effect of climate warming on epidemic dynamics. *Proceedings of the National
479 Academy of Sciences of the United States of America*, 115(4), 744–749. doi:
480 10.1073/pnas.1705067115
- 481 Greenspan, S. E., Bower, D. S., Webb, R. J., Roznik, E. A., Stevenson, L. A., Berger, L., Marantelli,
482 G., Pike, D. A., Schwarzkopf, L., & Alford, R. A. (2017). Realistic heat pulses protect frogs
483 from disease under simulated rainforest frog thermal regimes. *Functional Ecology*, 31(12),
484 2274–2286. doi: 10.1111/1365-2435.12944
- 485 Greenspan, Sasha E., Bower, D. S., Roznik, E. A., Pike, D. A., Marantelli, G., Alford, R. A.,
486 Schwarzkopf, L., & Scheffers, B. R. (2017). Infection increases vulnerability to climate change
487 via effects on host thermal tolerance. *Scientific Reports*, 7(1), 1–10. doi: 10.1038/s41598-017-
488 09950-3
- 489 Hall, S. R., Becker, C. R., Duffy, M. A., & Cáceres, C. E. (2010). Variation in resource acquisition

490 and use among host clones creates key epidemiological trade-offs. *American Naturalist*, 176(5),
491 557–565. doi: 10.1086/656523

492 Harvell, C. D., Montecino-Latorre, D., Caldwell, J. M., Burt, J. M., Bosley, K., Keller, A., Heron, S.
493 F., Salomon, A. K., Lee, L., Pontier, O., Pattengill-Semmens, C., & Gaydos, J. K. (2019).
494 Disease epidemic and a marine heat wave are associated with the continental-scale collapse of a
495 pivotal predator (*Pycnopodia helianthoides*). *Science Advances*, 5(1), 1–9. doi:
496 10.1126/sciadv.aau7042

497 Hector, T. E., Sgrò, C. M., & Hall, M. D. (2019). Pathogen exposure disrupts an organism’s ability to
498 cope with thermal stress. *Global Change Biology*, 25(11), 3893–3905. doi: 10.1111/gcb.14713

499 Hotez, P. J., Alvarado, M., Basáñez, M. G., Bolliger, I., Bourne, R., Boussinesq, M., Brooker, S. J.,
500 Brown, A. S., Buckle, G., Budke, C. M., Carabin, H., Coffeng, L. E., Fèvre, E. M., Fürst, T.,
501 Halasa, Y. A., Jasrasaria, R., Johns, N. E., Keiser, J., King, C. H., ... Naghavi, M. (2014). The
502 global burden of disease study 2010: interpretation and implications for the neglected tropical
503 diseases. *PLoS Neglected Tropical Diseases*, 8(7), e2865. doi: 10.1371/journal.pntd.0002865

504 Jacobs, A. F. G., Heusinkveld, B. G., Kraai, A., & Paaijmans, K. P. (2008). Diurnal temperature
505 fluctuations in an artificial small shallow water body. *Int J Biometeorol*, 52, 271–280. doi:
506 10.1007/s00484-007-0121-8

507 Kirk, D., Jones, N., Peacock, S., Phillips, J., Molnár, P. K., Krkošek, M., & Luijckx, P. (2018).
508 Empirical evidence that metabolic theory describes the temperature dependency of within-host
509 parasite dynamics. *PLoS Biology*, 16(2), e2004608. doi: 10.1371/journal.pbio.2004608

510 Kirk, D., Luijckx, P., Jones, N., Krichel, L., Pencer, C., Molnár, P. K., & Krkošek, M. (2020).
511 Experimental evidence of warming-induced disease emergence and its prediction by a trait-based
512 mechanistic model. *Proc. R. Soc. B*, 287, 20201526. doi: 10.1098/rspb.2020.1526

513 Kirk, D., Luijckx, P., Stanić, A., & Krkošek, M. (2019). Predicting the thermal and allometric
514 dependencies of disease transmission via the metabolic theory of ecology. *The American*
515 *Naturalist*, 193(5), 661–676.

516 Klüttgen, B., Dulmer, U., Engels, M., & Ratte, H. T. (1994). Adam, an artificial fresh-water for the
517 culture of zooplankton. *Water Research*, 28, 743–746.

- 518 Kuha, J., Arvola, L., Hanson, P. C., Huotari, J., Huttula, T., Järvinen, M., Kallio, K., Ketola, M.,
519 Kuoppamäki, K., Lohila, A., Paavola, R., Vuorenmaa, J., Winslow, L., Kuha, J., Arvola, L.,
520 Hanson, P. C., Huotari, J., Huttula, T., Juntunen, J., ... Paavola, R. (2016). Response of boreal
521 lakes to episodic weather-induced events. *Inland Waters*, 6(4), 523–534. doi: 10.1080/IW-
522 6.4.886
- 523 Landis, S. H., Kalbe, M., Reusch, T. B. H., & Roth, O. (2012). Consistent pattern of local adaptation
524 during an experimental heat wave in a pipefish-trematode host-parasite system. *PLoS ONE*, 7(1).
525 doi: 10.1371/journal.pone.0030658
- 526 Larsson, J. I. R., Ebert, D., & Vavra, J. (1997). Ultrastructural study and description of *Ordospora*
527 *colligata* gen. et Spa nov. (Microspora, Ordosporidae fam. nov.), a new microsporidian parasite
528 of *Daphnia magna* (Crustacea, Cladocera). *European Journal of Protistology*, 443, 432–443.
- 529 Lunn, D., Spiegelhalter, D., Thomas, A., & Best, N. (2009). The BUGS project: Evolution, critique
530 and future directions. *Statistics in Medicine*, 28(25), 3049–3067. doi: 10.1002/sim.3680
- 531 Miner, B. E., de Meester, L., Pfrender, M. E., Lampert, W., & Hairston, N. G. (2012). Linking genes
532 to communities and ecosystems: *Daphnia* as an ecogenomic model. *Proceedings of the Royal*
533 *Society B: Biological Sciences*, 279(1735), 1873–1882. doi: 10.1098/rspb.2011.2404
- 534 Murdock, C. C., Paaijmans, K. P., Bells, A. S., King, J. G., Hillyer, J. F., Read, A. F., & Thomas, M.
535 B. (2012). Complex effects of temperature on mosquito immune function. *Proceedings of the*
536 *Royal Society B: Biological Sciences*, 279(1741), 3357–3366. doi: 10.1098/rspb.2012.0638
- 537 Nelson, R., & Demas, G. E. (1996). Seasonal changes in immune function. *Review Literature And Arts*
538 *Of The Americas*, 71(4), 511–548.
- 539 Niehaus, A. C., Angilletta, M. J., Sears, M. W., Franklin, C. E., & Wilson, R. S. (2012). Predicting the
540 physiological performance of ectotherms in fluctuating thermal environments. *Journal of*
541 *Experimental Biology*, 215(4), 694–701. doi: 10.1242/jeb.058032
- 542 Paaijmans, K. P., Blanford, S., Bell, A. S., Blanford, J. I., Read, A. F., & Thomas, M. B. (2010).
543 Influence of climate on malaria transmission depends on daily temperature variation.
544 *Proceedings of the National Academy of Sciences*, 107(34), 15135–15139. doi:
545 10.1073/pnas.1006422107

- 546 Paaijmans, K. P., Heinig, R. L., Seliga, R. A., Blanford, J. I., Blanford, S., Murdock, C. C., & Thomas,
547 M. B. (2013). Temperature variation makes ectotherms more sensitive to climate change. *Global*
548 *Change Biology*, 19(8), 2373–2380. doi: 10.1111/gcb.12240
- 549 Paull, S. H., Raffel, T. R., Lafonte, B. E., & Johnson, P. T. J. (2015). How temperature shifts affect
550 parasite production: Testing the roles of thermal stress and acclimation. *Functional Ecology*,
551 29(7), 941–950. doi: 10.1111/1365-2435.12401
- 552 Plummer, M., Best, N., Cowles, K., & Vines, K. (2006). CODA: convergence diagnosis and output
553 analysis for MCMC - Open Research Online. *R News*, 6(1), 7–11.
- 554 R Core Team. (2018). *R: A language and environment for statistical computing*. Vienna, Austria: R
555 Foundation for Statistical Computing. Retrieved from <http://www.r-project.org/>.%0A
- 556 Raffel, T. R., Romanic, J. M., Halstead, N. T., McMahon, T. A., Venesky, M. D., & Rohr, J. R.
557 (2013). Disease and thermal acclimation in a more variable and unpredictable climate. *Nature*
558 *Climate Change*, 3(2), 146–151. doi: 10.1038/nclimate1659
- 559 Régnière, J., Powell, J., Bentz, B., & Nealis, V. (2012). Effects of temperature on development,
560 survival and reproduction of insects: Experimental design, data analysis and modeling. *Journal*
561 *of Insect Physiology*, 58(5), 634–647. doi: 10.1016/j.jinsphys.2012.01.010
- 562 Rohr, J. R., & Raffel, T. R. (2010). Linking global climate and temperature variability to widespread
563 amphibian declines putatively caused by disease. *Proceedings of the National Academy of*
564 *Sciences*, 107(18), 8269–8274. doi: 10.1073/pnas.0912883107
- 565 Rohr, J. R., Raffel, T. R., Blaustein, A. R., Johnson, P. T. J., Paull, S. H., & Young, S. (2013). Using
566 physiology to understand climate-driven changes in disease and their implications for
567 conservation. *Conservation Physiology*, 1(1), 1–15. doi: 10.1093/conphys/cot022
- 568 Roth, O., Kurtz, J., & Reusch, T. B. H. (2010). A summer heat wave decreases the
569 immunocompetence of the mesograzer, *Idotea baltica*. *Marine Biology*, 157(7), 1605–1611. doi:
570 10.1007/s00227-010-1433-5
- 571 Schär, C., Vidale, P. L., Lu, D., Frei, C., Scha, C., Liniger, M. A., & Appenzeller, C. (2004). The role
572 of increasing temperature variability in European summer heatwaves. *Nature*, 427(January), 1–4.
573 doi: 10.1038/nature02300

- 574 Schreven, S. J. J., Frago, E., Stens, A., De Jong, P. W., & Van Loon, J. J. A. (2017). Contrasting
575 effects of heat pulses on different trophic levels, an experiment with a herbivore-parasitoid
576 model system. *PLoS ONE*, *12*(4), 1–13. doi: 10.1371/journal.pone.0176704
- 577 Schwartz, T. S., Pearson, P., Dawson, J., Allison, D. B., & Gohlke, J. M. (2016). Effects of fluctuating
578 temperature and food availability on reproduction and lifespan. *Exp Gerontol.*, *86*, 62–72. doi:
579 10.1016/j.physbeh.2017.03.040
- 580 Shocket, M. S., Strauss, A. T., Hite, J. L., Šljivar, M., Civitello, D. J., Duffy, M. A., Cáceres, C. E., &
581 Hall, S. R. (2018). Temperature drives epidemics in a zooplankton-fungus disease system: A
582 trait-driven approach points to transmission via host foraging. *American Naturalist*, *191*(4), 435–
583 451. doi: 10.1086/696096
- 584 Stahlschmidt, Z. R., French, S. S., Ahn, A., Webb, A., & Butler, M. W. (2017). A simulated heat wave
585 has diverse effects on immune function and oxidative physiology in the corn snake (*Pantherophis*
586 *guttatus*). *Physiological and Biochemical Zoology*, *90*(4), 434–444. doi: 10.1086/691315
- 587 Uvarov, A. V., Tiunov, A. V., & Scheu, S. (2011). Effects of seasonal and diurnal temperature
588 fluctuations on population dynamics of two epigeic earthworm species in forest soil. *Soil Biology*
589 *and Biochemistry*, *43*(3), 559–570. doi: 10.1016/j.soilbio.2010.11.023
- 590 Vasseur, D. A., DeLong, J. P., Gilbert, B., Greig, H. S., Harley, C. D. G., McCann, K. S., Savage, V.,
591 Tunney, T. D., & O'Connor, M. I. (2014). Increased temperature variation poses a greater risk to
592 species than climate warming. *Proceedings of the Royal Society B: Biological Sciences*,
593 *281*(1779). doi: 10.1098/rspb.2013.2612
- 594 Zhang, Y. B., Yang, A. P., Zhang, G. F., Liu, W. X., & Wan, F. H. (2019). Effects of simulated heat
595 waves on life history traits of a host feeding parasitoid. *Insects*, *10*(12), 1–13. doi:
596 10.3390/insects10120419
- 597
- 598

599 Table S1: Priors for each of the parameters in the Beta Function for each of the different (j)
 600 temperature regimes (constant, fluctuating, heatwave) and life history traits (infection rate, spore
 601 burden, reproductive output) which were all drawn from the uniform distribution with specified limits.
 602 Priors for the minimum, optimal and maximum temperature satisfy the necessary condition
 603 $T_{min} \leq T_{opt} \leq T_{max}$ and were informed by previous work (Kirk et al., 2018, 2019). Priors for the scaling
 604 parameter F_m were restricted to be positive and less than ten on the log10 scale for both spore burden
 605 and host reproductive output and between 0 and 1 for infection rates. A Poisson likelihood was used
 606 for the observed reproductive output of the host and spore burden and the rate parameter λ was
 607 modelled as a function of temperature with a log link function, with different parameter values for
 608 each of the three temperature regimes. For infection rates we used a similar approach but using a
 609 binomial likelihood where the probability p was estimated from the beta function constrained so that 0
 610 $\leq p \leq 1$ and N was the number of *Daphnia* in each temperature regime.

parameter	Infection rate (min, max)	Spore burden (min, max)	Host reproductive output (min, max)
F_m [j]	0,1	0,10	0,10
T_{min} [j]	5, 15	5,14	0,14
T_{opt} [j]	T_{min} [j] + 0, T_{min} [j] + 20	T_{min} [j] + 0, T_{min} [j] + 10	T_{min} [j] + 0, T_{min} [j] + 25
T_{max} [j]	T_{opt} [j] + 0, 35	T_{opt} [j] + 0, 30	T_{opt} [j] + 0, 40

611
 612
 613 Table S2: Estimates of the parameters of the Beta Function for infection rate over the different
 614 temperature regimes. Provided are the mean thermal minimum (T_{min}), maximum (T_{max}) and thermal
 615 optimum (T_{opt}), as well as the maximum infection rate (F_m) with 95% confidence interval (lower CI,
 616 2.5% and upper 97.5%). The sample sizes for these estimates were respectively 82, 85 and 63 for
 617 constant, fluctuating and heat wave regimes.

Variable	Temperature regime	Infection status	Mean	CI 2.5%	CI 97.5%
F_m	constant	exposed	0.96	0.87	1.00
F_m	fluctuating	exposed	0.94	0.84	1.00
F_m	heat wave	exposed	0.95	0.85	1.00
T_{max}	constant	exposed	30.23	27.98	34.04
T_{max}	fluctuating	exposed	24.98	24.32	26.41
T_{max}	heat wave	exposed	29.49	24.96	34.56
T_{min}	constant	exposed	9.86	6.39	10.70
T_{min}	fluctuating	exposed	10.75	6.10	12.33
T_{min}	heat wave	exposed	10.88	5.42	13.79
T_{opt}	constant	exposed	19.72	18.13	21.27
T_{opt}	fluctuating	exposed	19.06	17.74	20.15
T_{opt}	heat wave	exposed	19.23	17.49	20.95

618
 619
 620

621 Table S3: Estimates of the parameters of the Beta Function for parasite burden over the different
 622 temperature regimes. Provided are the mean thermal minimum (T_{min}), maximum (T_{max}) and thermal
 623 optimum (T_{opt}), as well as the estimated number of spores at the thermal optimum (F_m) with their 95%
 624 confidence interval (lower CI, 2.5% and upper 97.5%). The sample sizes for these estimates were
 625 respectively 51, 46 and 46 for constant, fluctuating and heat wave regimes.

Variable	Temperature regime	Infection status	Mean	CI 2.5%	CI 97.5%
F_m	constant	exposed	489.78	478.63	501.19
F_m	fluctuating	exposed	467.74	446.68	478.63
F_m	heat wave	exposed	794.33	758.58	831.76
T_{max}	constant	exposed	27.70	27.45	27.95
T_{max}	fluctuating	exposed	24.80	24.52	25.07
T_{max}	heat wave	exposed	28.73	28.17	29.37
T_{min}	constant	exposed	11.49	10.75	12.11
T_{min}	fluctuating	exposed	11.48	10.18	12.32
T_{min}	heat wave	exposed	13.91	13.90	13.91
T_{opt}	constant	exposed	19.44	19.34	19.54
T_{opt}	fluctuating	exposed	19.30	19.23	19.39
T_{opt}	heat wave	exposed	15.76	15.53	15.97

626
627

628 Table S4: Estimates of the parameters of the Beta Function for the reproductive output of the host over
 629 the different temperature regimes. Provided are the mean thermal minimum (T_{min}), maximum (T_{max})
 630 and thermal optimum (T_{opt}), as well as the estimate for the highest reproductive output (F_m) with their
 631 and 95% confidence interval (lower CI, 2.5% and upper 97.5%). The sample size for these estimates
 632 were 81 and 81 for constant, 85 and 87 for fluctuating, and 64 and 61 for heat wave regimes for
 633 infected and uninfected individuals respectively.

Variable	Temperature regime	Infection status	Mean	CI 2.5%	CI 97.5%
F_m	constant	exposed	101.39	97.44	105.20
F_m	constant	unexposed	109.65	105.74	113.76
F_m	fluctuating	exposed	81.28	78.71	84.14
F_m	fluctuating	unexposed	106.41	102.85	110.15
F_m	heat wave	exposed	92.90	89.79	96.16
F_m	heat wave	unexposed	101.39	97.37	105.68
T_{max}	constant	exposed	36.22	35.37	37.16
T_{max}	constant	unexposed	37.58	36.73	38.51
T_{max}	fluctuating	exposed	38.90	36.54	39.97
T_{max}	fluctuating	unexposed	31.06	30.49	31.72
T_{max}	heat wave	exposed	39.46	38.11	39.99
T_{max}	heat wave	unexposed	34.68	30.79	39.38
T_{min}	constant	exposed	10.50	10.22	10.68
T_{min}	constant	unexposed	10.59	10.34	10.70
T_{min}	fluctuating	exposed	6.66	3.57	8.45
T_{min}	fluctuating	unexposed	0.63	0.02	2.18
T_{min}	heat wave	exposed	13.09	12.72	13.36
T_{min}	heat wave	unexposed	7.00	0.95	10.57
T_{opt}	constant	exposed	19.61	19.43	19.80
T_{opt}	constant	unexposed	20.22	20.05	20.39
T_{opt}	fluctuating	exposed	20.50	20.12	20.89
T_{opt}	fluctuating	unexposed	20.26	20.12	20.40
T_{opt}	heat wave	exposed	18.52	18.23	18.83
T_{opt}	heat wave	unexposed	21.16	20.74	21.69

634